A GEANT-based study of atmospheric neutrino oscillation parameters at INO

Abhijit Samanta,[1] Sudeb Bhattacharya,[1] Ambar Ghosal,[1] Kamales Kar,[1] Debasish Majumdar,[1] and Amitava Raychaudhuri[2,3]

[1]*Saha Institute of Nuclear Physics, 1/AF, Bidhannagar, Kolkata 700 064, India*
[2]*Harish-Chandra Research Institute, Chhatnag Road, Jhusi, Allahabad 211 019, India*
[3]*Department of Physics, University of Calcutta, 92 Acharya Prafulla Chandra Road, Kolkata 700 009, India*

(Dated: February 20, 2007)

We have studied the dependence of the allowed space of the atmospheric neutrino oscillation parameters on the time of exposure for a magnetized Iron CALorimeter (ICAL) detector at the India-based Neutrino Observatory (INO). We have performed a Monte Carlo simulation for a 50 kTon ICAL detector generating events by the neutrino generator NUANCE and simulating the detector response by GEANT. A chi-square analysis for the ratio of the up-going and down-going neutrinos as a function of L/E is performed and the allowed regions with the 90% and 99% CL are displayed. The possibilities of improvement and the uncertainties of the results have also been discussed.

PACS numbers: 14.60.Pq, 96.40.Tv

I. INTRODUCTION

The evidence of neutrino masses and their mixing[1] has brought neutrino physics into centre stage of particle physics. The neutrino mass eigenvalues and the Pontecorvo, Maki, Nakagawa, Sakata (PMNS) mixing matrix [2] connecting the mass to the flavor basis provides a natural framework for handling three active neutrinos.

The present information on the neutrino mass-squared differences and mixing angles are the following: From atmospheric neutrino detection one gets the best-fit values with 3σ error $|\Delta m^2_{23}| \simeq 2.5^{+.07}_{-0.6} \times 10^{-3}$ eV^2, $\sin^2\theta_{23} \simeq 0.5^{+0.18}_{-0.11}$ while solar neutrinos tell us $\Delta m^2_{12} \simeq 7.9 \times 10^{-5}$ eV^2, $\sin^2\theta_{12} \simeq 0.30$ [3]. Here we define $\Delta m^2_{ij} = m^2_j - m^2_i$.

At the moment, the sign of Δm^2_{23} is not known. The positive/negative value of this quantity denotes the direct/inverted mass ordering. The two large mixing angles and the mass squared differences may permit measurement of CP-violation in the lepton sector, if the third mixing angle, θ_{13}, and the CP phase, δ, are not too small. The current bound on the former is $\sin^2\theta_{13} < 0.05$ (3σ) [4, 5] while δ is unconstrained.

Thus the determination of mass hierarchy and the measurement of oscillation parameters with high precision is of utmost importance. The sensitivity of the measurement of a particular parameter depends crucially on the ranges of neutrino energy and path length traversed from the source to the detector. These ranges can be set in case of neutrino beams from artificial sources like nuclear reactors (energy $\sim$ MeV) and accelerators (energy $\sim$ GeV). The neutrinos with energy $\sim$ MeV (GeV) can also be obtained from natural sources like the sun (the atmosphere). Unlike typical accelerator or reactor neutrinos, the spectrum of atmospheric neutrinos covers many decades of energy ($E \sim 100$ MeV – few hundred GeV) with comparable interaction rate and baseline ($L \sim 10$ km - 12800 km). Since the oscillation probability depends mainly on L/E which varies in a wide range for atmospheric neutrinos, the measurement of the appearance/disappearance probability as a function of L/E can explore its variation over this entire range. This advantage is partly offset, however, by the difficulty that the flux is less known compared to that from man-made sources.

Currently around the world, there are many ongoing and planned experiments: MINOS[6], T2K[7], ICARUS[8], NOVA[9], D-CHOOZ[10], UNO[11], SKIII[12], Hyper-K[13], OPERA[14]. Out of these only MINOS employs a magnetic field and has a good charge identification capability. It is to be noted that all these experiments are planned in the northern hemisphere of the earth.

The proposed India-based Neutrino Observatory (INO) [15] at a site close to the equator plans to use a large magnetized Iron CALorimeter (ICAL) detector. The proposal is for an underground facility with more than 1 km overburden. Since it has a high charge identification capability ($> 90\%$)[15], it has a good chance of determining the neutrino mass ordering[16].

In this work we have studied the precision that can be achieved for $|\Delta m^2_{23}|$ and $\sin^2\theta_{23}$ at INO with atmospheric neutrinos. Obviously this depends on the exposure in terms of kTon-yr, reconstruction method, and the selection of the events in the analysis. The paper is organized as follows: A brief summary of the neutrino oscillation formalism is given in Section II. The ICAL detector at INO is described in Section III. In Section IV a brief account of the atmospheric neutrino flux that has been used in the present analysis has been

furnished. The generation of simulated data at ICAL and the analysis of such data are described in Section V. In Section VI we present the results and precision study of the oscillation parameters. Finally Section VII includes discussions and conclusions.

II. NEUTRINO OSCILLATION

A neutrino flavor eigenstate $|\nu_\alpha\rangle$ ($\alpha \equiv e,\mu,\tau$ etc.) in flavor basis can be written as a linear superposition of neutrino eigenstates $|\nu_i\rangle$ (with definite non-degenerate masses m_i) in mass basis given by $|\nu_\alpha\rangle = \sum_i U_{\alpha i}|\nu_i\rangle$ ($i = 1,2,3$ etc.). Here $U_{\alpha i}$ are the matrix elements of the neutrino mixing matrix U. This gives rise to the phenomenon of neutrino flavor oscillation. The probability that a neutrino ν_f with energy E gets converted into another neutrino ν_g after traversing a distance L in vacuum is given by

$$P(\nu_f \rightarrow \nu_g) = \delta_{fg} - 4\sum_{j>i} \mathrm{Re}(U^*_{fi}U_{gi}U_{fj}U^*_{gj}) \sin^2(1.27\Delta m^2_{ij}\frac{L}{E}) \pm 2\sum_{j>i} \mathrm{Im}(U^*_{fi}U_{gi}U_{fj}U^*_{gj}) \sin(2.54\Delta m^2_{ij}\frac{L}{E}) \quad (1)$$

In the above, L is expressed in km, E in GeV and Δm^2 in eV^2. The $-(+)$ refers to neutrinos (anti-neutrinos).

For a two-flavor scenario the above equation takes a simplified form given by

$$P_{\mathrm{survival}} = 1 - \sin^2 2\theta \sin^2(1.27\Delta m^2 \frac{L}{E}) \quad (2)$$

where θ is the mixing angle of neutrinos. Herein and in the rest of the paper the symbol θ and Δm^2 refer to θ_{32} and Δm^2_{32}.

III. THE INO DETECTOR

The simulation has been carried out for 50 kTon mass with dimension 48 m $\times$ 16 m $\times$ 12 m for the proposed magnetized Iron CALorimeter (ICAL) detector[15]. It consists of a stack of 140 horizontal layers of 6 cm thick iron slabs interleaved with 2.5 cm gap for the active detector elements. For the sake of illustration, we define a rectangular coordinate frame with origin at the center of the detector, $x(y)$-axis along the longest (shortest) lateral direction, and z-axis along the vertical direction. A magnetic field of strength 1 Tesla is considered along $+y$-direction. Resistive plate chambers (RPC) have been chosen as the active part of the detector. The readout of the RPCs is through the Cu strips having 2 cm width and placed orthogonally on the two external sides of the detectors. This type of detector has good time ($\sim$ 1 ns) and spatial resolutions.

IV. ATMOSPHERIC NEUTRINO FLUX

The atmospheric neutrinos are produced from the interactions of the cosmic rays with earth's atmosphere. The knowledge of the primary spectrum of cosmic rays has been improved from the observations by BESS[17] and AMS[18]. However, a large region of parameter space has been unexplored and they are interpolated or extrapolated from the measured flux. The difficulties and uncertainties in the calculation of the neutrino flux depends on the neutrino energy. The low energy flux is known quite well. The cosmic ray fluxes ($<$ 10 GeV) are modulated by solar activity and the geomagnetic field through a rigidity (momentum/charge) cutoff. At higher neutrino energy ($>$ 100 GeV), solar activity and rigidity cutoff are irrelevant[19]. There is an agreement within 5% among the calculations for neutrino energy below 10 GeV though different groups used different hadronic interaction models in their calculations.

We use the neutrino interaction cross section model of NUANCE [20] incorporating a typical Honda flux calculated in a 3-dimensional scheme[19].

V. DATA GENERATION AND METHOD OF ANALYSIS

The interactions of neutrinos with the detector material are simulated with the Monte Carlo method used in NUANCE[20]. In order to study the ICAL detector response for each event we use another Monte Carlo code GEANT[21]. The GEANT code uses the information of vertex position and momentum of the product particles obtained from the output of NUANCE simulation.

Event reconstruction: Our present analysis is based on the tracks generated by the muons that are produced by the charged current interactions of the neutrinos in the detector volume. The muons lose energy mainly due to ionization and radiative processes. This energy loss is proportional to the effective path-length which is the product of geometric path-length and the density of the media. This can be applied only for fully contained (FC) events.

In this simulation study we considered no atmospheric muon background and the noise hits produced by the detector. However, we conservatively assumed hits > 6 will be required for the reconstruction and filtering of the muon events from this background.

For a given triggered energy of a muon the number of hits decreases when one goes from vertical to horizontal direction since it traverses less number of active detector elements. However, this dependence on the direction is less for the ef-

fective path-length.

In case of partially contained (PC) events the momentum has been determined from the curvature of the track at the vertex in presence of the magnetic field applied across the detector. Due to our limitation of PC event reconstruction algorithm we considered PC events with hits < 20.

On the other hand, the hadrons produced create a shower of hits around the vertex of the event. *This implies that for any particular event the longest track normally comes from muons and this can be utilized for the analysis.*

The up-going muon type neutrinos traverse larger path-length undergoing oscillation whereas the down-going ones with much shorter path-length have little chance to oscillate. So one can visualize our detector set up as far (near) detector for the up-going (down-going) neutrinos. Then the ratio of up-going and down-going neutrinos (up/down) will act roughly as the survival probability. This up/down ratio as a function of L/E minimizes the systematic uncertainties in flux as well as in cross sections. The length L for the up-going neutrinos is the actual path-length traversed by them whereas for down-going neutrinos the reference path-length L is considered to be that of associated up-going neutrinos with zenith angle $(180^\circ - \theta_{\rm zenith})$ so that the range of L/E remains the same for up-going and down-going and down-going neutrinos [22].

Selection of events and Resolutions:

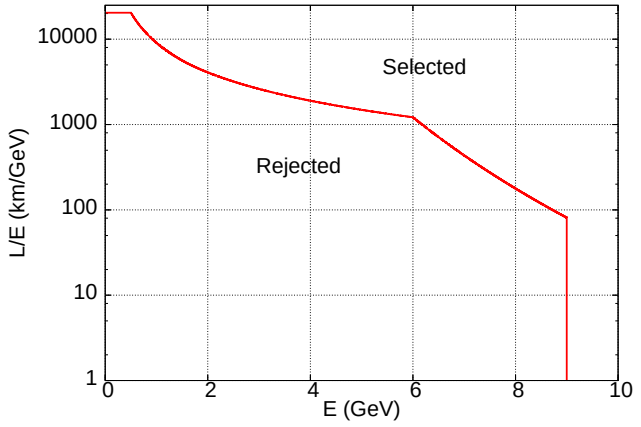

FIG. 1: The selection of events in $L/E - E$ plane with a good optimization between statistics and L/E resolution.

The L/E resolution has a complicated dependence on L and E. However, a few general remarks can be made here. Qualitatively for a fixed energy, the L resolution worsens gradually as we go from vertical to horizontal region and worsens rapidly close to the horizon. Also for a fixed direction, L/E resolution improves with increase in E. If one neglects totally the near horizon events (say, between zenith angle 70° and 110°) all the events below 200 km/GeV are lost. In our analysis we consider only the high energy events at near horizon and relax it gradually as we move away from the horizon. Quantitatively this is taken care of by an E dependent cut of the form :

$$L/E \geq aE^b$$

broken into three segments as shown in fig. 1.

Using the above cut the resolutions for E, L and L/E with atmospheric neutrino flux for the whole range of E_ν and L_ν are shown in fig. 2.

A representative statistics for 5 year data is shown in table I. Here the number of events with hits > 6 is considered for the analysis. Then this number is reduced after imposing the above E dependent L/E cut for a better resolution.

cut	Number of events survived			
	FC	efficiency	FC+PC	efficiency
hit>6 (for reconstruction)	4160	-	5351	-
E dependent L/E cut (for better L/E resolution)	2089	50.2%	2808	52.4%

TABLE I: Sample number of events after cuts in 5-year data for $\Delta m^2 = 2.3 \times 10^{-3}\text{eV}^2$.

Using the above cuts we find the up/down distribution for different time exposures of the ICAL detector. Here our main goal is to find how precisely one can measure Δm^2. A representative 'up/down' distribution with respect to L/E for 5 year FC events is shown in fig. 3. They are referred to as the 'experimental up/down' distributions.

χ^2-analysis:

In the χ^2-analysis the 'theoretical up/down' distribution is obtained by taking 40 years of atmospheric un-oscillated charged current muon neutrino data. The oscillation probability is then calculated from the neutrino L and E for each event and the event is kept or rejected by throwing a random number. We smear this over the whole range of L/E following the L/E-resolution function. Finally the up/down ratio is calculated for different L/E bins.

In this process we are also minimizing the effects due to the geomagnetic effect and the shape of the earth. However, at the high energy the geomagnetic effect is small.

Then a χ^2-fit is made with 'experimental up/down' distribution varying the atmospheric mass square difference Δm^2 and the mixing angle θ.

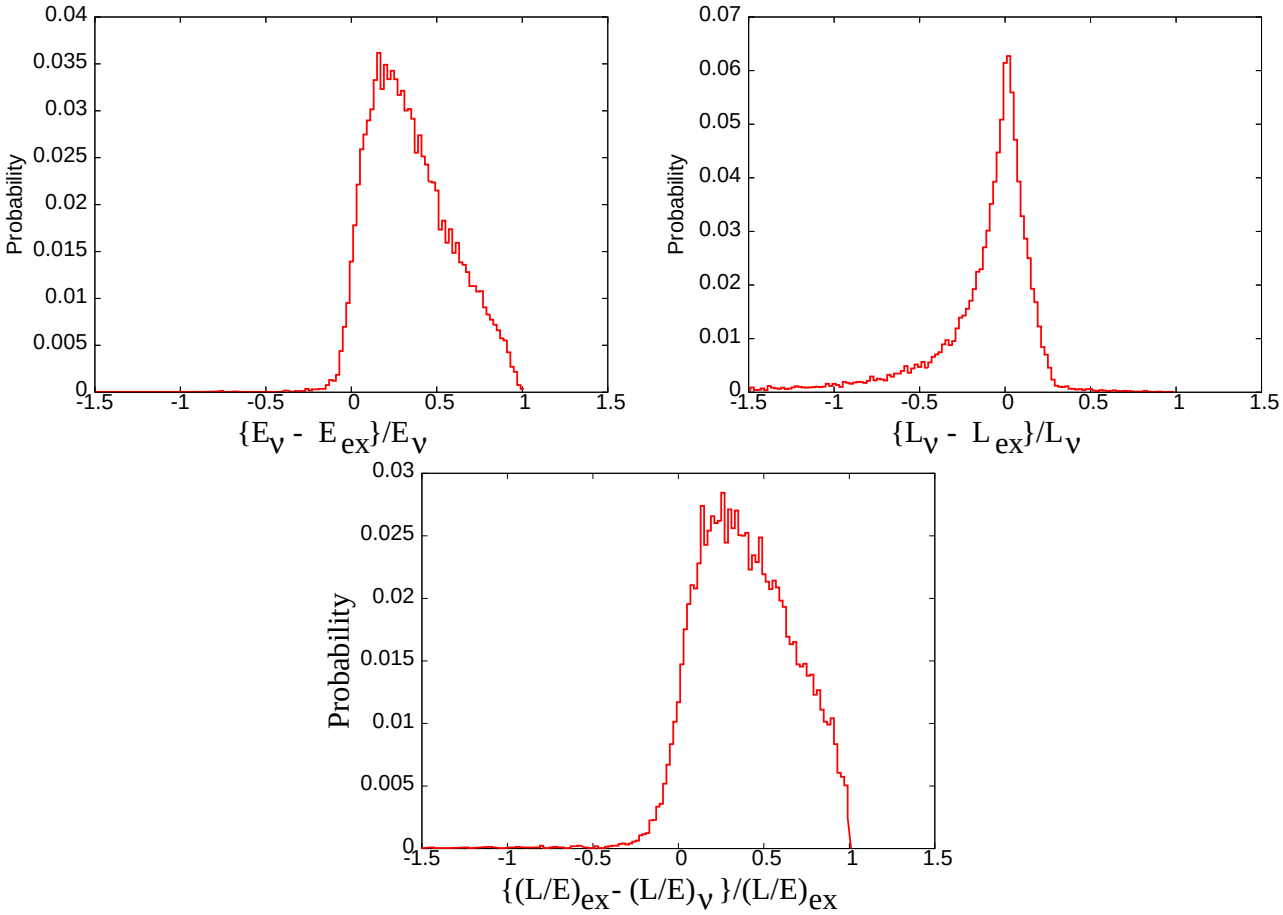

FIG. 2: The resolutions for E, L and L/E with atmospheric neutrino flux for whole range of E_ν and L_ν. The subscript 'ex' and ν refer to the reconstructed and true ν values.

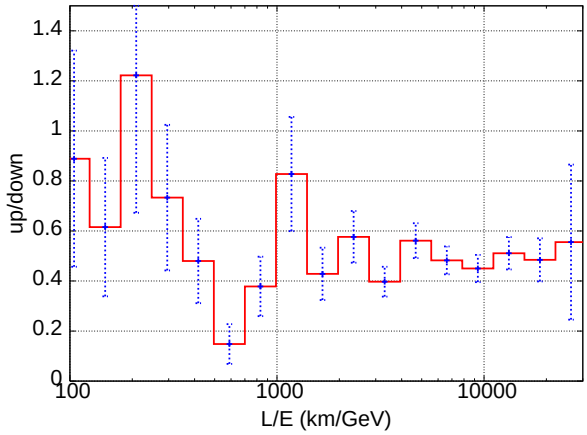

FIG. 3: The up/down distribution with L/E for 5 years FC events with $\Delta m^2 = 2.3 \times 10^{-3}\text{eV}^2$.

VI. RESULT

We show in fig. 4 the contours in the Δm^2 — $\sin^2 2\theta$ plane for 90% and 99% CL with 5 years FC (upper left) and FC+PC (upper right) events for the input value of $\Delta m^2 = 2.5 \times 10^{-3}\text{eV}^2$ and with 10 years FC events (lower) for $\Delta m^2 = 2.7 \times 10^{-3}\text{eV}^2$.

It is noted that the extracted best-fit values gradually become close to the input value of Δm^2 with increase of exposure time. For example the best-fit value is found to be

2.50, 2.40 (2.50, 2.34) $\times 10^{-3}$eV^2 in 5, 10 years FC (FC+PC) events for the input 2.3 $\times 10^{-3}$eV^2. For all these cases the best-fit values of $\sin^2 2\theta$ turns out to be 1 with the input value 1. Since FC+PC sample contains more high energy events than FC sample only and the E and L resolution are better for PC events, the best-fit values obtained from this analysis are closer to the input value. With a change of the input Δm^2 from 2.5 to 2.7 $\times 10^{-3}$eV^2 for 10 year FC samples, the best-fit changes to 2.46 to 2.68 $\times 10^{-3}$eV^2.

The position of the dip in this up/down distribution is indicative of the best-fit value of Δm^2 while the overall statistics determines the size of the allowed parameter space. Particularly, the statistics in the larger (smaller) L/E region from the dip determines the lower (upper) bound of Δm^2. For atmospheric neutrinos the statistics increases with increase of L/E thus resulting a lower bound in the contour of Δm^2.

A. Precision

We define precision (P) for a certain confidence level of a particular set of oscillation parameters as

$$\mathrm{P} = 2\left(\frac{\mathrm{UL}-\mathrm{LL}}{\mathrm{UL}+\mathrm{LL}}\right)$$

where 'UL' and 'LL' are the upper and lower limit of the contour respectively at the specified confidence level.

FC analysis: The variation of precision of $\sin^2\theta$ and Δm^2 with different years of exposure is shown separately in fig. 5 at 90% and 99% CL. It is seen that the precision falls very slowly beyond 10 years and that can be a useful observation for the future experiment.

It is further observed that the precision gradually becomes worse when we increase the value of Δm^2 from 2.3×10^{-3}eV^2. This is demonstrated in fig. 6.

The reason behind this is the following. The position of the dip in the up/down distribution shifts towards large value of L/E with the decrease of the value Δm^2. The flux increases rapidly with decrease of energy and the statistics becomes gradually high at larger L/E.

However, we comment that there is a competition between statistics and L/E resolution. We see that at low value of Δm^2, say 2.1 $\times 10^{-3}$eV^2, the precision worsens compared to that at 2.3 $\times 10^{-3}$eV^2. This can be improved if we choose more stringent cuts with good L/E resolution for larger values of L/E. So one has to optimize between the requirement of statistics and L/E-resolution, which depends mainly on the range of interest of Δm^2.

FC+PC analysis: After the inclusion of the PC events the results are very similar to that obtained from FC events and hence are not shown separately.

VII. DISCUSSIONS

Simulation studies for atmospheric neutrinos at the proposed Iron Calorimeter (ICAL) detector at INO have been made with a goal to determine the level of precision which may be achieved. The oscillated atmospheric neutrino events for a known set of values of oscillation parameters are generated with an event generator code namely NUANCE and the simulated signals in the detector is obtained through a detector simulation code namely GEANT that uses the NUANCE output as its inputs. A chi-square analysis of the results obtained analyzing this simulated GEANT output data properly chosen using appropriate constraints ("cuts") (designated as "Experimental Data") is then carried out by varying the oscillation parameters within certain ranges and thereby producing sets of oscillated NUANCE outputs for these parameters. These outputs (designated as "Theoretical Data") are in fact used for the chi-square analysis and subsequently for the precision studies.

There are, however, scopes for improvements of these studies.

- The present analysis is performed only with the simulated muon signals neglecting the hadrons. The estimation of neutrino energy E and L/E from only muon tracks is, therefore, more conservative than that obtained including hadrons. As mentioned earlier hadrons mainly produce showers instead of well defined tracks (clean signal such as for muons) and thus the present method is not effective to extract energy information (or directional information) from such hadron showers. A new methodology is to be developed for this purpose and this work of incorporating hadrons in the analysis is in progress and will be reported in future.

- Here we have made a two-flavor analysis whereas more realistic approach would be the analysis of a simulated data following a full three-flavor oscillation formalism.

- For the analysis of PC events the curvature of the track is used for calculation of energy. In the high energy regime the tracks have no or negligible curvature inside the detector volume and hence such PC events could not be considered in the present analysis. These PC events, if considered, would have increased the statistics.

Moreover, we find the resolutions are energy dependent and significantly different for neutrinos and anti-neutrinos. One

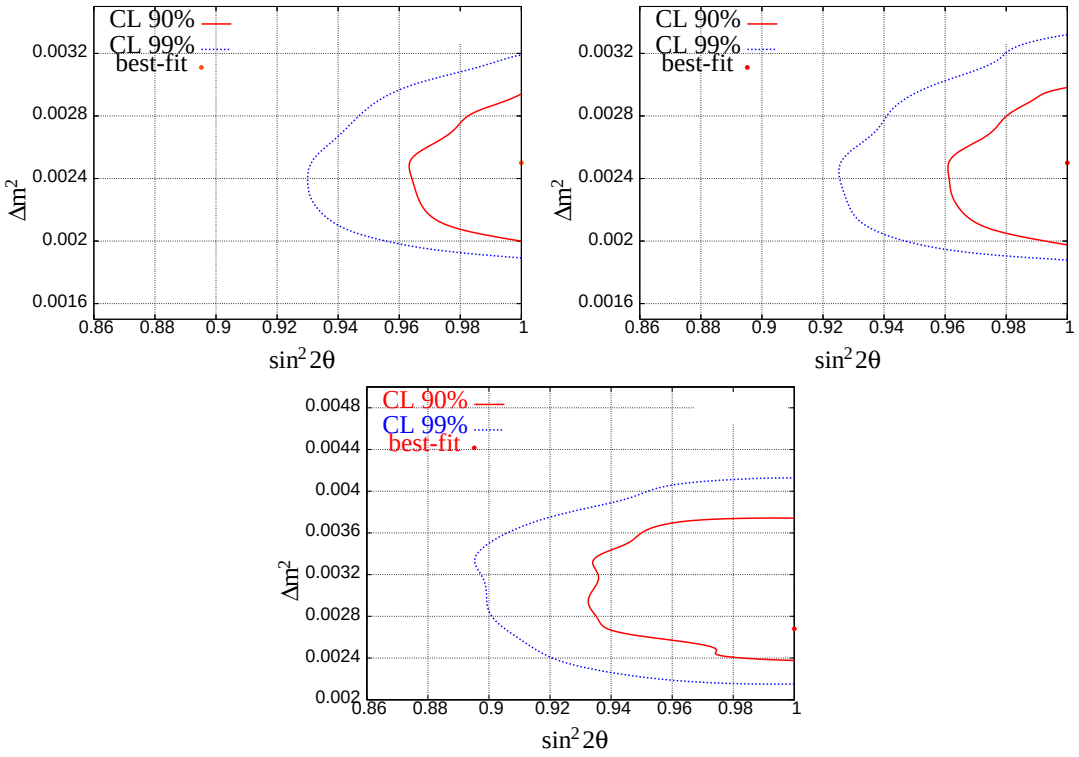

FIG. 4: The contour plots in Δm^2 — $\sin^2 2\theta$ plane with 5 years FC events (upper left), FC+PC event (upper right) for $\Delta m^2 = 2.3 \times 10^{-3}\text{eV}^2$ and with 10 years FC events for $\Delta m^2 = 2.7 \times 10^{-3}\text{eV}^2$(lower).

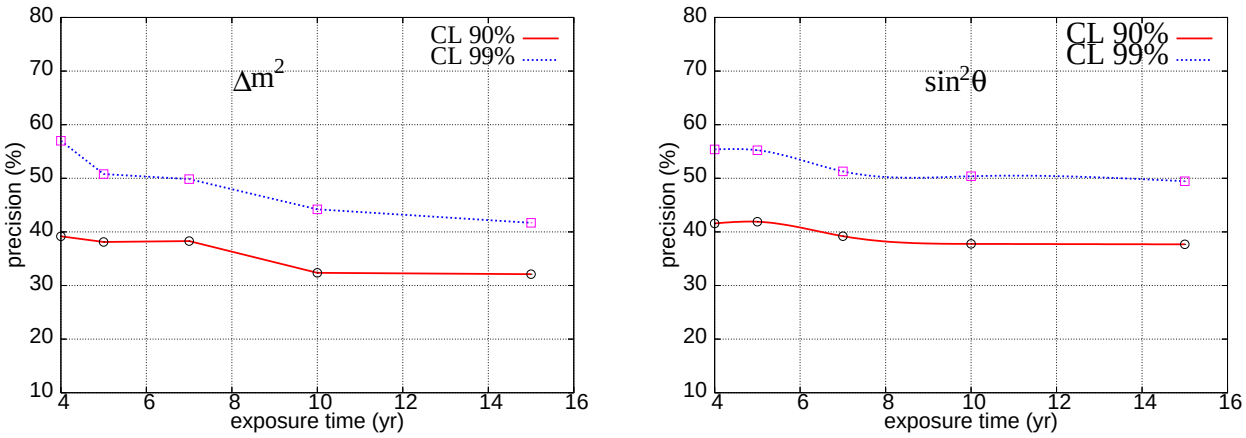

FIG. 5: The variation of the precision of Δm^2 (left) and $\sin^2\theta$ (right) with time of exposure for 50kTon ICAL with FC events for the input of $\Delta m^2 = 2.3 \times 10^{-3}\text{eV}^2$.

therefore expects to obtain more precise best fit values with C.L. contours in parameter space further shrinked, if one uses a multiple resolution functions, instead of one as used here. In doing so, the whole $L - E$ plane is divided into multiple small segments (mesh) and separate resolution functions are obtained for each such segment of the mesh which is then used for the purpose of analysis.

Acknowledgements

The authors thank Gobinda Majumder, Subhendu Rakshit, Sunanda Banerjee, Subhashis Chattopadhyay and Naba K Mondal for their help and valuable suggestions at different phases of the work.

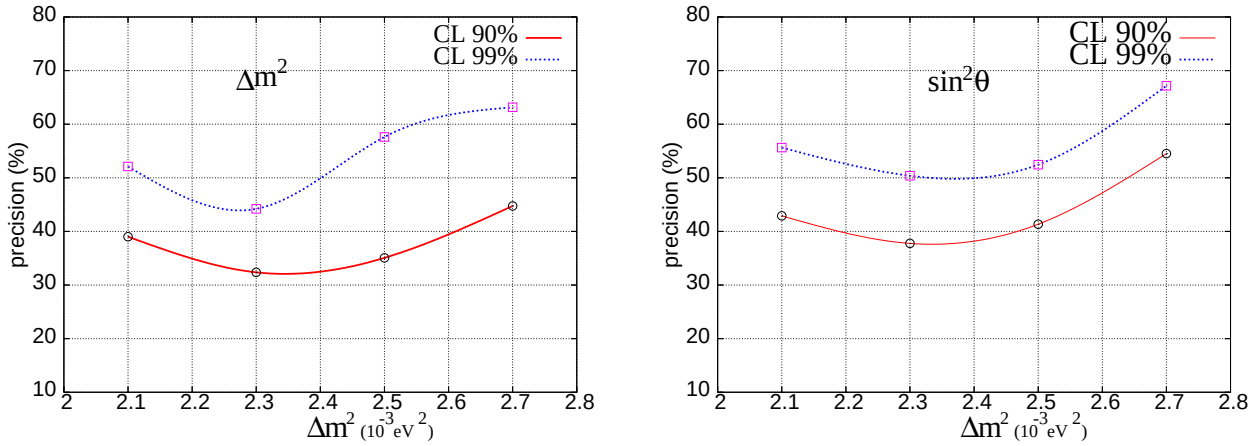

FIG. 6: The variation of the precision of Δm^2 (left) and $\sin^2\theta$ (right) with the input value of Δm^2 for 50kTon ICAL with 10 years FC events.

[1] Review of Particle Physics, S. Eidelman *et al.*, Phys. Lett. **B 592** (2004) 1.

[2] B. Pontecorvo, JETP **6** (1958) 429; **7** (1958) 172; Z. Maki, M. Nakagawa and S. Sakata, Prog. Theor. Phys. **28**, 870 (1962).

[3] T. Schwetz, Phys. Scripta **T127**, 1 (2006) [arXiv:hep-ph/0606060].

[4] M. Apollonio *et al.* [CHOOZ Collaboration], Phys. Lett. B **466**, 415 (1999) [arXiv:hep-ex/9907037].

[5] A. Bandyopadhyay, S. Choubey, S. Goswami, S. T. Petcov and D. P. Roy, Phys. Lett. B **608**, 115 (2005) [arXiv:hep-ph/0406328].

[6] M. G. Zois, FERMILAB-MASTERS-2004-06

[7] Y. Yamada [T2K Collaboration], Nucl. Phys. Proc. Suppl. **155**, 207 (2006).

[8] J. Kisiel [ICARUS Collaboration], Acta Phys. Polon. B **36**, 3227 (2005).

[9] R. Ray, Nucl. Phys. Proc. Suppl. **154**, 179 (2006).

[10] G. Horton-Smith [Double Chooz Collaboration], AIP Conf. Proc. **805**, 142 (2006).

[11] C. K. Jung, arXiv:hep-ex/0005046.

[12] H. Back *et al.*, arXiv:hep-ex/0412016.

[13] K. Nakamura, Int. J. Mod. Phys. A **18**, 4053 (2003).

[14] F. Di Capua [OPERA Collaboration], PoS **HEP2005**, 177 (2006).

[15] V. Arumugam *et al.* [INO Collaboration], INO-2005-01

[16] D. Indumathi and M. V. N. Murthy, Phys. Rev. D **71**, 013001 (2005) [arXiv:hep-ph/0407336]; S. T. Petcov and T. Schwetz, Nucl. Phys. B **740**, 1 (2006) [arXiv:hep-ph/0511277]; A. Samanta, arXiv:hep-ph/0610196.

[17] T. Maeno *et al.* [BESS Collaboration], Astropart. Phys. **16**, 121 (2001) [arXiv:astro-ph/0010381].

[18] J. Alcaraz *et al.* [AMS Collaboration], Phys. Lett. B **461**, 387 (1999) [arXiv:hep-ex/0002048].

[19] M. Honda, T. Kajita, K. Kasahara and S. Midorikawa, Phys. Rev. D **70**, 043008 (2004) [arXiv:astro-ph/0404457].

[20] D. Casper, Nucl. Phys. Proc. Suppl. **112**, 161 (2002) [arXiv:hep-ph/0208030].

[21] GEANT Detector Simulation and Simulation Tool, CERN Program Library Long Write-up W5013, March 1994, http://wwwasd.web.cern.ch/wwwasd/cernlib/version.html

[22] P. Picchi and F. Pietropaolo, ICGF RAP. INT. 344/1997, Torino 1997 (CERN preprint SCAN-9710037).